HHS Public Access

Author manuscript

Nat Chem Biol. Author manuscript; available in PMC 2015 September 01.

Published in final edited form as:

Nat Chem Biol. 2015 March ; 11(3): 201–206. doi:10.1038/nchembio.1732.

Coordinated gripping of substrate by subunits of a AAA+ proteolytic machine

Ohad Iosefson[1], **Andrew R. Nager**[1], **Tania A. Baker**[1,2], and **Robert T. Sauer**[1,*]

[1]Department of Biology, Massachusetts Institute of Technology, Cambridge, MA 02139

[2]Howard Hughes Medical Institute, Massachusetts Institute of Technology, Cambridge, MA 02139

Abstract

Hexameric AAA+ unfoldases of ATP-dependent proteases and protein-remodeling machines use conserved loops that line the axial pore to apply force to substrates during the mechanical processes of protein unfolding and translocation. Whether loops from multiple subunits act independently or coordinately in these processes is a critical aspect of mechanism but is currently unknown for any AAA+ machine. By studying covalently linked hexamers of the *E. coli* ClpX unfoldase bearing different numbers and configurations of wild-type and mutant pore loops, we show that loops function synergistically, with the number of wild-type loops required for efficient degradation depending upon the stability of the protein substrate. Our results support a mechanism in which a power stroke initiated in one subunit of the ClpX hexamer results in the concurrent movement of all six pore loops, which coordinately grip and apply force to the substrate.

AAA+ enzymes (ATPases associated with varied cellular activities) are ubiquitous molecular machines that perform mechanical work in all cells[1]. For example, AAA+ proteases and protein-remodeling machines remove damaged or unneeded proteins, resolubilize aggregates, and/or disassemble macromolecular complexes in bacterial, archaeal, and eukaryotic cells[2]. In most ATP-dependent proteases and protein-remodeling machines, a AAA+ ring hexamer binds a target protein and then unfolds it by translocation through a narrow axial pore. In AAA+ proteases, the denatured polypeptide is translocated into a self-compartmentalized peptidase for degradation. In the ClpXP protease, for example, ClpX is the AAA+ ring hexamer, and ClpP is the peptidase. ClpXP degradation begins with ClpX recognition of a specific peptide tag or degron, cycles of ATP hydrolysis pull the tag through a narrow axial pore and unfold the attached protein, and then additional cycles of ATP hydrolysis drive polypeptide translocation into the ClpP chamber (Fig. 1a)[3].

ATP-fueled changes in the conformation of the *E. coli* ClpX ring cause movement of Tyr^{153}-Val^{154}-Gly^{155} loops, which line the axial translocation pore[4–9]. All AAA+ hexamers

*corresponding author: bobsauer@mit.edu.

AUTHOR CONTRIBUTIONS O.I. and A.R.N. designed and performed experiments; all authors analyzed data and contributed to writing the manuscript.

The authors declare no competing financial interests

that translocate and unfold proteins contain related axial-pore loops, with strong conservation of an aromatic Tyr (Y), Trp (W), or Phe (F) side chain at the first position (Fig. 1b). The aromatic side chains in one or more of these ClpX pore loops bind the degradation tag as the machine pulls the attached native substrate through the axial channel, forcing its denaturation[5–6]. Once unfolding is successful, axial pore-loop movement coupled to conformational changes in the ClpX ring propel the translocating polypeptide through the pore in steps of 5–8 residues per power stroke, facilitating processive degradation[6,10–14]. In ClpX and other homohexameric AAA+ unfoldases and protein remodeling machines, substitution of the bulky aromatic side chain with a small alanine (A) side chain in each subunit eliminates detectable degradation *in vivo* and *in vitro*[4,15–21].

Despite the central importance of axial-pore loops in AAA+ proteases and protein-remodeling machines, almost nothing is known about potential coordination among these loops during unfolding and/or translocation. Do individual pore loops act independently or do loops from multiple subunits cooperate in unfolding or translocating the substrate? Here, we address these questions by studying the activities of ClpX variants with different numbers and configurations of wild-type and mutant axial-pore loops. We find that neighboring loops function in a synergistic or coordinated manner, with the number of wild-type loops required for efficient degradation depending on the resistance of the protein substrate to mechanical unfolding. Variants with as few as three wild-type loops degrade an unfolded substrate as fast or faster than the wild-type enzyme, but more wild-type loops are required to unfold and degrade increasingly resistant native substrates. Based on these results, we propose and discuss evidence for a mechanism in which ATP hydrolysis in a single subunit results in a power stroke in which all six pore loops concurrently move, grip, and coordinately apply an unfolding force to the protein substrate.

Results

Hexamers with mixtures of mutant and wild-type pore loops

Mutations were introduced into genes encoding six covalently linked *E. coli* $ClpX^{\Delta N}$ subunits to generate pseudo hexamers with amino-acid sequence changes in specific subunits or combinations of subunits[22]. We constructed and purified covalent pseudo hexamers containing from one to six mutant AVG pore loops. For enzymes with two to four mutant poor loops, we also generated and purified variants with the mutant and wild-type subunits in different configurations (Fig. 2a). We refer to the covalent hexamer with six wild-type loops (Y153) as YYYYYY, the hexamer with six mutant loops (A153) as $_{AAAAAA}$, and hexamers with a mixture of mutant and wild-type loops by names such as $_{A}Y_{A}YYY$ (mutations in subunits 1 and 3 of the hexamer) and $_{A}YY_{A}YY$ (mutations in subunits 1 and 4 of the hexamer).

As observed previously for wild-type ClpX[23], each ClpX variant hydrolyzed ATP in the absence of protein substrate and addition of ClpP reduced the hydrolysis rate (Fig. 2b; Supplementary Results, Supplementary Table 1), with the latter observation confirming a functional interaction between ClpP and each ClpX variant. In general, the rate of ATP hydrolysis increased with the number of mutant pore loops whether or not ClpP was present (Fig. 2b). There is evidence that the wild-type axial pore of ClpX is normally tightly packed

and that the slow step in ATP hydrolysis is a conformational change[9,24]. Thus, the pore-loop mutants probably accelerate the rate of ATP hydrolysis by accelerating the rate-limiting conformational change, either because the mutant pores are packed less tightly[6] and/or because the mutations remove or weaken restricting contacts made by the wild-type Y153 side chains. If relief of tight packing and reduced axial-pore volume were the only reason for the increase in ATP hydrolysis by the mutants, then variants with Y153L mutations should have lower ATPase rates than otherwise identical Y153A variants, as leucine is intermediate in size/volume between tyrosine and alanine. To test this possibility, we constructed, purified, and assayed rates of basal ATP hydrolysis by $_{L}$YYYYY, $_{LL}$YYYY, $_{LLL}$YYY, and $_{LLLL}$YY ClpX$^{\Delta N}$ variants. As shown in Fig. 2c, each leucine variant had a higher ATPase rate than the corresponding alanine variant. Thus, the increased ATPase rates of the pore-loop variants do not scale with reduced size or volume of the mutant side chains, and interference with restrictive contacts made by wild-type Y153 side chains is likely to be responsible, at least in part, for faster ATP hydrolysis in these variants.

Degradation of an unfolded substrate

To determine how the number and configuration of wild-type and mutant pore loops contribute to substrate recognition and translocation, we measured degradation of increasing concentrations of ^{UF}titin^{I27}-ssrA, a domain unfolded by chemical modification of buried cysteines with an ssrA tag to target it to ClpX[25] (Fig. 3a; Supplementary Fig. 1). For YYYYYY, $_{A}$YYYYY, $_{AA}$YYYY, $_{A}$Y$_{A}$YYY, $_{A}$YY$_{A}$YY, $_{AAA}$YYY, $_{AA}$Y$_{A}$YY, $_{A}$Y$_{A}$Y$_{A}$Y, and $_{AAAA}$YY ClpXP, there was enough curvature in plots of the degradation rate versus the substrate concentration to determine K_M and V_{max} values by fitting to the Michaelis-Menten equation (Fig. 3a–c; Supplementary Fig. 1; Supplementary Table 2). K_M for these variants increased substantially as the number of wild-type pore loops decreased (Fig. 3b), suggesting that multiple wild-type pore loops participate in ssrA-tag binding. For $_{AA}$Y$_{AA}$Y, $_{AAA}$Y$_{A}$Y, $_{AAAAA}$Y, and $_{AAAAAA}$ ClpXP, the rate of degradation of the unfolded protein varied linearly with substrate concentration (Fig. 3a; Supplementary Fig. 1), a result expected if most of these mutant ClpXP enzymes are not substrate bound. This behavior indicated a K_M in excess of 80 μM, the highest concentration of substrate tested, but precluded determination of individual K_M and V_{max} values. However, the slope of each line is equal to V_{max}/K_M, the second-order rate constant for degradation. V_{max}/K_M values for the complete set of Y153A variants spanned a ~200-fold range and decreased as the number wild-type pore loops decreased (Fig. 3d). Notably, however, the degradation activities of mutants with three or four mutant pore loops varied considerably.

Intriguingly, V_{max} for degradation of ^{UF}titin^{I27}-ssrA by the $_{A}$YYYYY, $_{AA}$YYYY, $_{A}$Y$_{A}$YYY, $_{A}$YY$_{A}$YY, $_{AAA}$YYY, and $_{AA}$Y$_{A}$YY ClpXP variants was similar to or faster than the wild-type value (Fig. 3c). After calculating the energetic efficiency of degradation by dividing the maximal degradation rate by the rate of ATP hydrolysis in the presence of ClpP and saturating protein substrate (Supplementary Fig. 2), we found that degradation by $_{AAA}$YYY and $_{AA}$Y$_{A}$YY ClpXP required only 50–60% as much ATP as degradation by YYYYYY ClpXP (Supplementary Table 2).

$_{A}$Y$_{A}$Y$_{A}$Y ClpXP degradation of the ^{UF}titin^{I27}-ssrA substrate was ~15-fold slower and used ~14-fold more ATP than $_{AAA}$YYY ClpXP degradation (Fig. 3c; Supplementary Table 2), indicating that the configuration of functional pore loops plays an important role in the speed and energetic efficiency of proteolysis or that this configuration of mutant pore loops interferes with ClpP binding. We found, however, that the apparent affinity of $_{A}$Y$_{A}$Y$_{A}$Y ClpX for ClpP was within error of the wild-type affinity (Supplementary Fig. 3). Other ClpX variants that displayed low degradation activity ($_{AAA}$Y$_{A}$Y, $_{AA}$Y$_{AA}$Y, $_{AAAAA}$Y; and $_{AAAAAA}$) also bound ClpP well enough (Supplementary Fig. 3) to ensure that ClpXP complexes were efficiently assembled at the enzyme concentrations used for degradation assays. Unlike $_{AAA}$YYY and other variants that mediated rapid ^{UF}titin^{I27}-ssrA degradation, $_{A}$Y$_{A}$Y$_{A}$Y contains no adjacent wild-type loops, suggesting that adjacent functional pore loops mediate more efficient degradation. In support of this model, V_{max}/K_{M} for ClpXP degradation of ^{UF}titin^{I27}-ssrA was roughly similar for all variants containing no adjacent wild-type pore loops ($_{A}$Y$_{A}$Y$_{A}$Y, $_{AAA}$Y$_{A}$Y, $_{AA}$Y$_{AA}$Y, $_{AAAAA}$Y, and $_{AAAAAA}$) (Supplementary Table 2). In combination, these results reveal that a full complement of wild-type pore loops is not required for ClpXP recognition of the ssrA tag, for substrate engagement, or for translocation and degradation of unfolded substrates, although different geometric arrangements of wild-type and mutant pore loops can have substantial effects on the overall degradation rate and on the amount of ATP hydrolyzed.

In single-chain ClpX hexamers, the first and sixth subunits differ from the remaining subunits in being covalently linked to just one other subunit. Because ClpX functions as a topologically closed ring[8], the relative positions of wild-type and mutant pore loops in any given variant should define its properties rather than their positions relative to the first and sixth subunits. To test this assumption, we assayed degradation of ^{UF}titin^{I27}-ssrA by Y$_{A}$YY$_{A}$Y and YY$_{A}$YY$_{A}$ ClpXP, which contain the same relative configuration of wild-type and mutant pore loops as $_{A}$YY$_{A}$YY ClpXP but in different orders with respect to the termini of the covalent hexamer. Each enzyme degraded different concentrations of this substrate at essentially the same rate (Fig. 3e), supporting the importance of relative rather than absolute configuration. Thus, the arrangements of wild-type and mutant pore loops shown in Fig. 2a are representative of all possible configurations.

Unfolding and degradation of increasingly stable proteins

We challenged the pore-loop variants with derivatives of green fluorescent protein (GFP) or superfolder GFP (^{SF}GFP) that were increasingly difficult to unfold and degrade (Fig. 4a–c, Supplementary Fig. 4). cp7-^{SF}GFP-ssrA, a circularly permuted variant, is relatively easy to unfold, GFP-ssrA is more difficult, and ^{SF}GFP-ssrA is the most difficult[26]. The $_{A}$YYYYY, $_{AA}$YYYY, $_{A}$Y$_{A}$YYY, $_{A}$YY$_{A}$YY, $_{AAA}$YYY, and $_{AA}$Y$_{A}$YY ClpXP enzymes supported cp7-^{SF}GFP-ssrA degradation with V_{max} values that were 94%, 62%, 63%, 62%, 39%, and 8% of the YYYYYY value, respectively, whereas $_{A}$Y$_{A}$Y$_{A}$Y and variants with two or fewer wild-type loops failed to degrade this substrate (Fig. 4a; Supplementary Fig. 4; Supplementary Table 2). Thus, cp7-^{SF}GFP-ssrA unfolding and degradation activity requires at least three wild-type pore loops and becomes more efficient as the number of wild-type poor loops increases.

Pore-loop configuration was an important factor both in determining the rate and ATP cost of cp7-^{SF}GFP-ssrA degradation (Fig. 4a,d; Supplementary Table 2). For example, $_{AAA}$YYY ClpXP degraded this substrate with a ~5-fold higher V_{max} and ~4-fold lower ATP cost than the isomeric $_{AA}$Y$_{A}$YY ClpXP (Fig. 4a; Supplementary Table 2). Notably, $_{AAA}$YYY and $_{AA}$Y$_{A}$YY ClpXP degraded the unfolded titin substrate with similar maximal rates and ATP costs (Fig. 4d; Supplementary Table 2), suggesting that $_{AA}$Y$_{A}$YY ClpXP requires many more power strokes than $_{AAA}$YYY ClpXP to unfold cp7-^{SF}GFP-ssrA. Thus, configurations of wild-type pore loops that mediate similar rates of degradation of an unfolded substrate can have substantially different unfolding activities.

Wild-type ClpXP unfolds and degrades GFP-ssrA more slowly than cp7-^{SF}GFP-ssrA[26]. V_{max} for degradation of GFP-ssrA by $_{A}$YYYYY ClpXP was ~65% of the YYYYYY ClpXP value and consumed roughly twice as much ATP per substrate, whereas V_{max} for the $_{AA}$YYYY, $_{A}$YY$_{A}$YY, and $_{A}$Y$_{A}$YYY variants was ~10% of wild type and the ATP costs were ~10-fold higher (Supplementary Table 2; Fig. 4b,d; Supplementary Fig. 4). No degradation of this difficult protein substrate was observed using variants with three or fewer wild-type pore loops.

$_{A}$YYYYY ClpXP degraded ^{SF}GFP-ssrA, which is more stable than GFP-ssrA[26], at ~50% of the YYYYYY rate and used about twice as much ATP, whereas $_{AA}$YYYY and other variants with fewer than five wild-type pore loops failed to degrade this substrate (Supplementary Table 2; Fig. 4c,d; Supplementary Fig. 4). Together, these results show that successful unfolding of increasingly resistant substrates requires the coordinated action of a greater number of wild-type pore loops. Moreover, if unfolding can be successfully achieved using fewer wild-type pore loops, then the energetic cost of degradation is substantially higher in terms of the number of ATP molecules hydrolyzed per substrate degraded.

Independence of pore-loop and ATP-hydrolysis mutations

To probe the linkage between pore-loop function and ATP hydrolysis, we assayed GFP-ssrA degradation by ClpXP variants containing a single Y153A mutation ($_{A}$YYYYY), a single E185Q mutation in the Walker-B motif that results in an ATP-hydrolysis defect[27] (Y^{EQ}YYYYY), both mutations in the same subunit ($_{A}$^{EQ}YYYYY), and each mutation in a different subunit ($_{A}$Y^{EQ}YYYY). V_{max} for GFP-ssrA degradation by $_{A}$YYYYY ClpXP and by Y^{EQ}YYYYY ClpXP was 67% and 35%, respectively, of the value for YYYYYY ClpXP (Fig. 5). Thus, the ATP-hydrolysis mutation causes a greater defect than the pore-loop mutation. If pore-loop function requires ATP hydrolysis in the same subunit, then $_{A}$^{EQ}YYYYY ClpXP should be no less active than Y^{EQ}YYYYY ClpXP, but this was not the case. V_{max} for GFP-ssrA degradation by $_{A}$^{EQ}YYYYY ClpXP was 10.5% of the YYYYYY value, and V_{max} for $_{A}$Y^{EQ}YYYY was 8.4% of this value (Fig. 5). Together, these results indicate that a combination of an ATP-hydrolysis mutation and a pore-loop mutation have roughly the same effects on degradation whether they are present in the same or different subunits. This outcome is inconsistent with a model in which a given pore loop only applies an unfolding force to the substrate when ATP is hydrolyzed in the same subunit and is in accord with studies showing that pore-loop mutations in hydrolytically inactive ClpX subunits reduce degradation efficiency[6].

Pore-loop defects slow the initial step in unfolding

ClpX unfolds GFP-ssrA and ^{SF}GFP-ssrA by initially extracting β-strand 11, which is the element of secondary structure adjacent to the ssrA tag, then denaturing the resulting 10-stranded β-barrel, and finally translocating the rest of the fully denatured substrate into ClpP for degradation[5,13,26,]. The initial strand-extraction reaction can be studied using a split substrate produced by thrombin cleavage between β-strands 10 and 11 (called ^{SF}GFP-10/11-ssrA), as extraction of the terminal β11 strand reduces fluorescence induced by excitation with 400-nm light[26]. YYYYYY ClpXP extracted the β11-ssrA element roughly twice as fast as $_{A}$YYYYY, whereas the $_{AA}$YYYY variant was inactive in extraction (Fig. 6a). Thus, the reductions in ClpXP degradation of ^{SF}GFP-ssrA caused by mutating one or two axial pore loops correlate with defects in the initial strand-extraction reaction (Fig. 6b).

To test if $_{AA}$YYYY ClpXP could extract β11-ssrA from a split GFP substrate in which packing interactions with flanking β strands were destabilized by mutations, we cloned, purified, and prepared a split ^{SF}GFP-10/11-ssrA substrate bearing the F223A and A226G mutations in β-strand 11. These mutations alter the ratio of fluorescence resulting from excitation with 400-nm and 467-nm light, and thus direct comparisons with the Fig. 6a experiment are not informative. Nevertheless, $_{AA}$YYYY ClpXP was only slightly less active than $_{A}$YYYYY ClpXP in extracting the ssrA-tagged F223A/A226G β11 strand of the destabilized split ^{SF}GFP substrate (Fig. 6c). These results support a model in which the number of wild-type pore loops needed to initiate unfolding depends on the stability of structural elements proximal to the degron tag.

Discussion

Studies in solution and at the single-molecule level show that ClpX pulls on a substrate using power strokes driven by the ATPase cycle[6,11–14,22,25]. For unstructured polypeptide substrates, these pulling events lead to translocation in discrete steps of approximately 1, 2, 3, or 4 nm, with steps longer than 1 nm resulting from a rapid burst of coordinated ATP-hydrolysis events and power strokes. There is no repeating step-size pattern[14], suggesting that ATP hydrolysis in different subunits of the ClpX ring occurs stochastically rather than in a required sequence. Supporting a non-sequential mechanism, ClpX variants with only one or two ATPase-functional subunits are active in protein degradation[22]. For a native protein substrate, denaturation appears to occur when a power stroke coincides with transient thermal destabilization of structure near the substrate degron, and thus a very large number of power strokes can be required before unfolding is successful[11–14,25].

How many ClpX pore loops move and apply force to the substrate during a power stroke initiated by ATP hydrolysis in a single subunit? One possibility is that just the pore loop in the hydrolyzing subunit grips the substrate, moves, and is responsible for the power stroke, with subsequent power strokes mediated by ATP hydrolysis in other subunits of the AAA+ ring resulting in a hand-over-hand translocation mechanism. Another proposal is that two subunits on opposite sides of the hexameric ring of a different AAA+ unfoldase are responsible for gripping and executing a power stroke, with additional pairs of opposed subunits mediating subsequent power strokes[28]. For models like these, in which only one or two pore loops grip the substrate at a time, ClpXP degradation activity should vary almost

linearly with the number of functional pore loops, as futile power strokes that move non-functional loops would simply add proportionally to the overall degradation time or ATP cost. Our results, however, show non-linear activities as the number of wild-type pore loops changes. For example, $_{A}$YYYYY ClpXP has one more wild-type pore loop than $_{AA}$YYYY ClpXP but degrades GFP-ssrA ~7-fold faster and using ~7-fold less ATP. In addition, our results do not support models in which just two opposed subunits or three alternating subunits in the hexamer grip the substrate. Thus, $_{AAA}$YYY (no opposed wild-type loops) is quite active in degrading cp7-^{SF}GFP-ssrA, the $_{AA}$Y$_{A}$YY isomer (one pair of opposed wild-type loops) is ~5-fold less active, and the $_{A}$Y$_{A}$Y$_{A}$Y isomer (one set of three alternating wild-type loops) is inactive.

We propose a model in which every pore loop in the ClpX hexamer concurrently grips the substrate, moves, and applies force during a power stroke resulting from a single ATP hydrolysis event. Our coordinated pore-loop gripping and movement model is consistent with the general architecture of the topologically closed ClpX ring, which consists of six rigid-body units connected by six hinges[7–9]. Each rigid-body unit contains a single pore loop that would move, albeit with some flexibility, in concert with its rigid body. Moreover, the conformation of the hinge in nucleotide-bound subunits is sensitive to whether ATP or ADP is bound. Thus, ATP hydrolysis in a single subunit could alter the conformation of the local hinge, and this conformational change would propagate around the ring via the flanking rigid-body units, providing a mechanism to coordinate concurrent movement of all six pore loops. There are no substrate-bound structures of ClpX[7,9] but one analogous to the AAA+ Rpt$_{1–6}$ unfolding ring of the 26*S* proteasome[29] would allow all six pore loops to contact a translocating polypeptide. Following a power stroke, other regions of the axial pore may constrict and clamp the substrate to maintain grip on the substrate and prevent slipping as the pore loops reset for the next power stroke.

Our coordinated gripping model provides an explanation for current and previous experiments[6] in which pore-loop mutations in ATPase-defective subunits affect degradation by ClpXP. Specifically, pore loops in subunits that are not actively hydrolyzing ATP would still grip and help apply mechanical force to a substrate, and thus mutations in these loops could alter the efficiency of degradation. Indeed, we find that the combined effects on protein degradation of a pore-loop mutation and an ATP-hydrolysis mutation are similar whether these mutations are in the same ClpX subunit or in different subunits.

Our model also explains the requirement for larger numbers of wild-type pore loops for ClpXP to unfold and degrade increasingly difficult protein substrates. For example, we find that at least three wild-type pore loops are required to unfold/degrade the least stable native substrate tested (cp7-^{SF}GFP-ssrA), at least four wild-type loops are needed to degrade the next most difficult substrate (GFP-ssrA), and at least five wild-type loops are necessary to degrade the most resistant substrate (^{SF}GFP-ssrA). Moreover, $_{A}$YYYYY ClpXP extracts the ssrA-tagged strand of a split ^{SF}GFP-10/11-ssrA substrate and degrades ^{SF}GFP-ssrA more slowly than YYYYYY ClpXP, as predicted if each pore loop in the wild-type enzyme contributes to gripping and performing mechanical work on these substrates. Why is better gripping, mediated by more wild-type pore loops, linked to the success of enzymatic unfolding of increasingly stable substrates? As ClpX translocation of a substrate degron

begins to deform a native protein, a force equal and opposite to the unfolding force works to break enzyme-substrate contacts. Whether the protein denatures or slips from the grasp of ClpX will depend on its stability and how tightly it is bound. Indeed, previous experiments established that ClpX frequently releases stable native substrates during failed unfolding attempts[10], and we find that the ATP cost of ClpXP unfolding and degradation can increase by 10-fold or more as protein substrate stability increases and the number of wild-type ClpX pore loops decreases. The latter result indicates that most power strokes fail to unfold GFP substrates when grip strength is reduced.

Changes in grip strength could also explain the observation that *E. coli* ClpXP fails to unfold and degrade ^{SF}GFP-ssrA, GFP-ssrA, and cp7-^{SF}GFP-ssrA when ATP concentrations and rates of hydrolysis are low[5,26]. For example, low ATP concentrations could result in a weaker grip if pore loops in ATP-free subunits are more flexible than those in ATP-bound subunits. It has been proposed that GFP is not unfolded at low ATP concentrations because ClpXP predominantly takes 2-nm translocation steps and fails to take longer steps under these conditions[13]. However, a related AAA+ protease, ClpAP, only takes 1- and 2-nm translocation steps at saturating concentrations of ATP but unfolds GFP faster than ClpXP[30]. Moreover, *Mycobacterium tuberculosis* ClpXP has very low hydrolysis activity at saturating concentrations of ATP but still unfolds and degrades GFP-ssrA[31]. In combination, these results suggest that ClpX grips substrates most tightly with an ATP-saturated hexameric ring and a full complement of wild-type pore loops.

Translocation of an unfolded substrate in solution is not opposed by a substantial force and is an easier mechanical task than unfolding a natively folded protein. Indeed, ClpX pore-loop variants that do not unfold any of the native substrates tested still degrade unfolded ^{UF}titin^{I27}-ssrA. We find, however, that the rate of degradation of ^{UF}titin^{I27}-ssrA also depends on the number and configuration of wild-type pore loops, with some mutants degrading this substrate faster than wild-type ClpXP. Some of this increase in degradation rate appears to result from faster ATP hydrolysis by these mutants. Surprisingly, however, $_{AAA}$YYY ClpXP degrades one molecule of ^{UF}titin^{I27}-ssrA using approximately half as many molecules of ATP (28 ± 2) as wild-type ClpXP (54 ± 3). Rates of solution degradation by ClpXP are slower than expected based on rates of single-molecule unfolding and/or translocation, suggesting that engagement or commitment is the slow step in degradation and requires the largest number of power strokes[14]. Thus, $_{AAA}$YYY ClpXP may initiate degradation more efficiently than the wild-type enzyme. A less likely possibility is that $_{AAA}$YYY ClpXP translocates more residues per power stroke than wild-type ClpXP.

Why might a mutant with fewer wild-type pore loops be able to engage a substrate more rapidly? Based on crystal structures, the axial pore in substrate-free ClpX appears to be closed as a consequence of packing between pore loops[7]. Moreover, mutational and crosslinking studies suggest that RKH loops surrounding the entrance to the axial pore engage the ssrA degron weakly in a first step of binding, with the YVG and pore-2 loops mediating tighter binding in a second binding step in which the degron moves more deeply into the pore[32]. Creation of an open translocation channel may be easier in the less tightly packed pores of some mutants, requiring fewer power strokes to move a weakly bound ssrA degron into the pore. However, the pore of the $_{A}$Y$_{A}$Y$_{A}$Y isomer should also be less tightly

packed but this ClpXP variant degrades ^{UF}titin^{I27}-ssrA almost ~15-times slower and at a correspondingly higher ATP cost than $_{AAA}$YYY ClpXP. $_{A}$Y$_{A}$Y$_{A}$Y ClpXP is also less active and uses more ATP than $_{AAAA}$YY ClpXP, suggesting a special role for adjacent wild-type pore loops, either in efficient initiation or in translocation. For example, neighboring wild-type pore loops might contact adjacent portions of the substrate, allowing loop-loop contacts as well as loop-substrate contacts to contribute to productive engagement or translocation.

Online Methods

Proteins and biochemical assays

E. coli ClpP, single-chain *E. coli* ClpX variants, and ssrA-tagged GFP substrates were expressed as described[22,26,33]. Briefly, proteins were purified by Ni^{+2}-NTA (Qiagen) affinity chromatography, desalted into a low ionic strength buffer on a PD-10 column (GE Healthcare), purified further by ion-exchange chromatography, run on a HiLoad 16/60 Superdex 200 size-exclusion column (Amersham), and stored frozen at −80 °C in PD buffer (25 mM HEPES, pH 7.6, 100 mM KCl, 20 mM $MgCl_2$, 10% glycerol (v/v)). Degradation assays were performed at 30 °C in PD buffer supplemented with 4 mM ATP and a regeneration system consisting of 16 mM creatine phosphate (MP Biomedicals) and 0.32 mg/mL creatine phosphokinase (Sigma). GFP degradation and extraction of the ssrA-tagged strand of split ^{SF}GFP-10/11-ssrA were quantified by loss of 511-nm fluorescence after excitation at 400 or 467 nm[26]. Rates of ATP hydrolysis were determined using an NADH coupled assay in PD buffer at 30 °C[34]. The binding of ClpX variants to ClpP was assayed by changes in the rate of cleavage of a decapeptide[35].

Preparation and degradation of unfolded titin^{I27}

An ssrA-tagged variant of the titin^{I27} domain was unfolded by chemical modification of two cysteines in the hydrophobic core[25,36]. For purification, a plasmid encoding Y9P His_6-tagged titin^{I27}-ssrA[25], was transformed into *E. coli* X90, cells were grown at 37 °C to an OD_{600} of 0.6, 1 mM IPTG was added, and the temperature was lowered to 25 °C for additional 3 h of growth. After harvesting, the pellet from 1.5 L of culture was suspended in 15 mL of buffer A (100 mM NaH_2PO_4, 50 mM Tris base, 6 M guanidine hydrochloride, 20 mM imidazole, 0.1 mM EDTA, 10 mM β-mercaptoethanol, pH 8.0), incubated for 30 min at room temperature and then transferred to −80 °C for 45 min. The frozen cells were thawed, and 30 mL of buffer A was added. After an additional 30 min incubation at room temperature, the cells were lysed by sonication and centrifuged for 45 min at 14000 rpm. The soluble fraction was mixed with Ni-agarose beads that had been pre-equilibrated with buffer A (~4 ml beads volume) at room temperature for 45 min. The beads were washed three times with buffer A, transferred to an empty gravity-flow column (Bio-Rad), washed with 10 mL of buffer B (100 mM NaH_2PO_4, 50 mM Tris base, 5 M guanidine hydrochloride, 20 mM imidazole, 150 mM NaCl, 0.1 mM EDTA, 10 mM β-mercaptoethanol, pH 8.5), and then washed then with 10 mL of buffer C (50 mM Tris base, 5 M guanidine hydrochloride, 20 mM imidazole, 150 mM NaCl, 0.1 mM EDTA, pH 8.0). Bound proteins were eluted from the column with 10 mL of buffer D (50 mM Tris base, 5 M guanidine hydrochloride, 350 mM imidazole, 150 mM NaCl, pH 8.0). Fractions of 1 mL were collected, aliquots were tested with Bradford reagent (Bio-Rad), and those containing

protein were pooled. For labeling, 5-iodoacetamidofluorescein (Pierce Biotechnology) dissolved in N,N-dimethyl formamide was added at a five-fold molar excess over protein, the mixture was incubated in the dark for two h at room temperature, and the sample was desalted into PD buffer using a PD-10 column (GE Healthcare). As a final purification step, the sample was chromatographed on a HiLoad 16/60 Superdex 200 column (Amersham) in PD buffer at 4 °C. Fractions containing fluorescent ^{UF}titin^{I27}-ssrA were concentrated, divided into aliquots, and flash frozen in liquid N_2. The circular-dichroism spectrum of the ^{UF}titin^{I27}-ssrA protein (10 μM in phosphate buffered saline, pH 7.4) taken on an AVIV Model 420 Spectrometer at room temperature was characteristic of a random-coil protein. The concentration of fluorescein modified ^{UF}titin^{I27}-ssrA was determined using the protein Bradford assay (Bio-Rad). Non-fluorescent ^{UF}titin^{I27}-ssrA was prepared using a similar protocol, except that cysteines were modified with iodoacetamide (Sigma) present at a 100-fold molar excess over protein.

^{UF}titin^{I27}-ssrA degradation experiments were performed in PD buffer without glycerol, fluorescently labeled ^{UF}titin^{I27}-ssrA was mixed with a 5.5 molar excess of non-fluorescent ^{UF}titin^{I27}-ssrA, and proteolysis was assayed by monitoring the changes in fluorescence anisotropy (excitation 480 nm; emission 520 nm). A sample of ^{UF}titin^{I27}-ssrA (5 μM) was incubated with excess ClpXP (2 μM ClpX; 3 μM ClpP) for 30 min and the final anisotropy value was used to define complete proteolysis. Assays were performed using a SpectraMax M5 micro-plate reader (Molecular Devices).

Supplementary Material

Refer to Web version on PubMed Central for supplementary material.

ACKNOWLEDGEMENTS

This work was supported by NIH grant GM-101988 (R.T.S.). T.A.B. is an employee of the Howard Hughes Medical Institute. We thank Karl Schmitz and Eyal Gur for materials, advice, and helpful discussions.

References

1. Ogura T, Wilkinson AJ. AAA+ superfamily ATPases: common structure--diverse function. Genes Cells. 2001; 6:575–597. [PubMed: 11473577]
2. Sauer RT, Baker TA. AAA+ proteases: ATP-fueled machines of protein destruction. Annu. Rev. Biochem. 2011; 80:587–612. [PubMed: 21469952]
3. Baker TA, Sauer RT. ClpXP, an ATP-powered unfolding and protein-degradation machine. Biochim. Biophys. Acta. 2012; 1823:15–28. [PubMed: 21736903]
4. Siddiqui SM, Sauer RT, Baker TA. Role of the protein-processing pore of ClpX, an AAA+ ATPase, in recognition and engagement of specific protein substrates. Genes Dev. 2004; 18:369–374. [PubMed: 15004005]
5. Martin A, Baker TA, Sauer RT. Protein unfolding by a AAA+ protease is dependent on ATP-hydrolysis rates and substrate energy landscapes. Nat. Struct. Mol. Biol. 2008; 15:139–145. [PubMed: 18223658]
6. Martin A, Baker TA, Sauer RT. Pore loops of the AAA+ ClpX machine grip substrates to drive translocation and unfolding. Nat. Struct. Mol. Biol. 2008; 15:1147–1151. [PubMed: 18931677]
7. Glynn SE, Martin A, Nager AR, Baker TA, Sauer RT. Structures of asymmetric ClpX hexamers reveal nucleotide-dependent motions in a AAA+ protein-unfolding machine. Cell. 2009; 139:744–756. [PubMed: 19914167]

8. Glynn SE, Nager AR, Baker TA, Sauer RT. Dynamic and static components power unfolding in topologically closed rings of a AAA+ proteolytic machine. Nat. Struct. Mol. Biol. 2012; 19:616–622. [PubMed: 22562135]
9. Stinson BM, et al. Nucleotide binding and conformational switching in the hexameric ring of a AAA+ machine. Cell. 2013; 153:628–639. [PubMed: 23622246]
10. Kenniston JA, Baker TA, Sauer RT. Partitioning between unfolding and release of native domains during ClpXP degradation determines substrate selectivity and partial processing. Proc. Natl. Acad. Sci. USA. 2005; 102:1390–1395. [PubMed: 15671177]
11. Aubin-Tam M-E, Olivares AO, Sauer RT, Baker TA, Lang MJ. Single-molecule protein unfolding and translocation by an ATP-fueled proteolytic machine. Cell. 2011; 145:257–267. [PubMed: 21496645]
12. Maillard RA, et al. ClpX(P) generates mechanical force to unfold and translocate its protein substrates. Cell. 2011; 145:459–469. [PubMed: 21529717]
13. Sen M, et al. The ClpXP protease unfolds substrates using a constant rate of pulling but different gears. Cell. 2013; 155:636–646. [PubMed: 24243020]
14. Cordova JC, et al. Stochastic but highly coordinated protein unfolding and translocation by the ClpXP proteolytic machine. Cell. 2014; 158:647–658. [PubMed: 25083874]
15. Song HK, et al. Mutational studies on HslU and its docking mode with HslV. Proc. Natl. Acad. Sci. USA. 2000; 97:14103–14108. [PubMed: 11114186]
16. Yamada-Inagawa T, Okuno T, Karata K, Yamanaka K, Ogura T. Conserved pore residues in the AAA protease FtsH are important for proteolysis and its coupling to ATP hydrolysis. J. Biol. Chem. 2003; 278:50182–50187. [PubMed: 14514680]
17. Hinnerwisch J, Fenton WA, Furtak KJ, Farr GW, Horwich AL. Loops in the central channel of ClpA chaperone mediate protein binding, unfolding, and translocation. Cell. 2005; 121:1029–1041. [PubMed: 15989953]
18. Graef M, Langer T. Substrate specific consequences of central pore mutations in the *i*-AAA protease Yme1 on substrate engagement. J. Struct. Biol. 2006; 156:101–108. [PubMed: 16527490]
19. Okuno T, Yamanaka K, Ogura T. Characterization of mutants of the *Escherichia coli* AAA protease, FtsH, carrying a mutation in the central pore region. J. Struct. Biol. 2006; 156:109–114. [PubMed: 16563799]
20. Rothballer A, Tzvetkov N, Zwickl P. Mutations in p97/VCP induce unfolding activity. FEBS Lett. 2007; 581:1197–1201. [PubMed: 17346713]
21. Zhang F, et al. Structural insights into the regulatory particle of the proteasome from *Methanocaldococcus jannaschii*. Mol. Cell. 2009; 34:473–484. [PubMed: 19481527]
22. Martin A, Baker TA, Sauer RT. Rebuilt AAA + motors reveal operating principles for ATP-fuelled machines. Nature. 2005; 437:1115–1120. [PubMed: 16237435]
23. Kim YI, et al. Molecular determinants of complex formation between Clp/Hsp100 ATPases and the ClpP peptidase. Nat. Struct. Biol. 2001; 8:230–233. [PubMed: 11224567]
24. Barkow SR, Levchenko I, Baker TA, Sauer RT. Polypeptide translocation by the AAA+ ClpXP protease machine. Chem. Biol. 2009; 16:605–612. [PubMed: 19549599]
25. Kenniston JA, Baker TA, Fernandez JM, Sauer RT. Linkage between ATP consumption and mechanical unfolding during the protein processing reactions of an AAA+ degradation machine. Cell. 2003; 114:511–520. [PubMed: 12941278]
26. Nager AR, Baker TA, Sauer RT. Stepwise unfolding of a β-barrel protein by the AAA+ ClpXP protease. J. Mol. Biol. 2011; 413:4–16. [PubMed: 21821046]
27. Hersch GL, Burton RE, Bolon DN, Baker TA, Sauer RT. Asymmetric interactions of ATP with the AAA+ $ClpX_6$ unfoldase: allosteric control of a protein machine. Cell. 2005; 121:1017–1027. [PubMed: 15989952]
28. Smith DM, Fraga H, Reis C, Kafri G, Goldberg AL. ATP binds to proteasomal ATPases in pairs with distinct functional effects, implying an ordered reaction cycle. Cell. 2011; 144:526–538. [PubMed: 21335235]
29. Matyskiela ME, Lander GC, Martin A. Conformational switching of the 26S proteasome enables substrate degradation. Nat. Struct. Mol. Biol. 2013; 20:781–788. [PubMed: 23770819]

30. Olivares AO, Nager AR, Yosefson O, Sauer RT, Baker TA. Mechanochemical basis of protein degradation by a double-ring AAA+ machine. Nat. Struct. Mol. Biol. 2014; 21:871–875. [PubMed: 25195048]

31. Schmitz KR, Sauer RT. Substrate delivery by the AAA+ ClpX and ClpC1 unfoldases activates the mycobacterial ClpP1P2 peptidase. Mol. Micro. 2014; 93:617–628.

32. Martin A, Baker TA, Sauer RT. Diverse pore loops of the AAA+ ClpX machine mediate unassisted and adaptor-dependent recognition of ssrA-tagged substrates. Mol. Cell. 2008; 29:441–450. [PubMed: 18313382]

33. Martin A, Baker TA, Sauer RT. Distinct static and dynamic interactions control ATPase-peptidase communication in a AAA+ protease. Mol. Cell. 2007; 27:41–52. [PubMed: 17612489]

34. Burton RE, Siddiqui SM, Kim YI, Baker TA, Sauer RT. Effects of protein stability and structure on substrate processing by the ClpXP unfolding and degradation machine. EMBO J. 2001; 20:3092–3100. [PubMed: 11406586]

35. Lee ME, Baker TA, Sauer RT. Control of substrate gating and translocation into ClpP by channel residues and ClpX binding. J. Mol. Biol. 2010; 399:707–718. [PubMed: 20416323]

36. Gur E, Sauer RT. Degrons in protein substrates program the speed and operating efficiency of the AAA+ Lon proteolytic machine. Proc. Natl. Acad. Sci. USA. 2009; 106:18503–18508. [PubMed: 19841274]

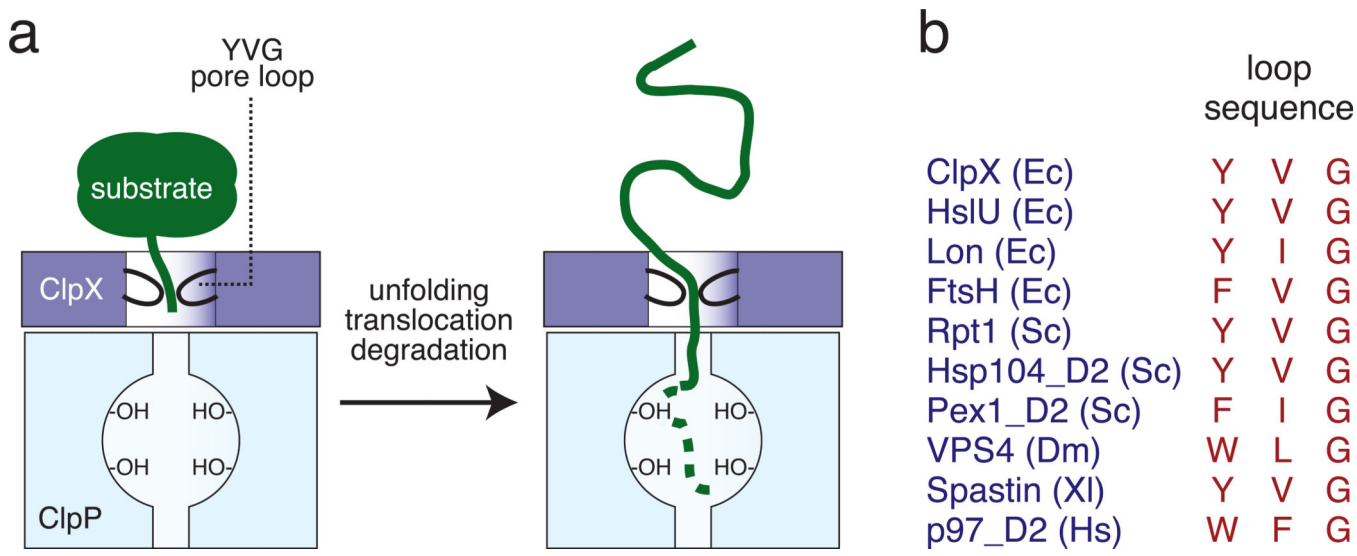

Figure 1.

Conserved loops in the axial pore of ClpX and related AAA+ machines mediate translocation and unfolding of polypeptide substrates. (**a**) YVG pore loops in the ClpX hexamer contact the degradation tag of a protein substrate and are thought to drive unfolding and translocation of the denatured polypeptide into the lumen of ClpP, a self-compartmentalized serine protease, for degradation. (**b**) The axial pore loops in AAA+ enzymes related to ClpX have an aromatic residue at the first loop position (Y, tyrosine; F, phenylalanine; W, tryptophan), a hydrophobic residue at the second position (V, valine; I, isoleucine; L, leucine, F, phenylalanine), and a glycine (G) at the third position. Ec, *Escherichia coli*; Sc, *Saccharomyces cerevisiae*; Dm, *Drosophila melanogaster*; Xl, *Xenopus leavis*; Hs, *Homo sapiens*. The Hsp104 and p97 disaggregating and unfolding machines and the Pex1 peroxisomal biogenesis factor contain D1 and D2 AAA+ rings; the pore-loop sequences shown are for the D2 rings of these enzymes.

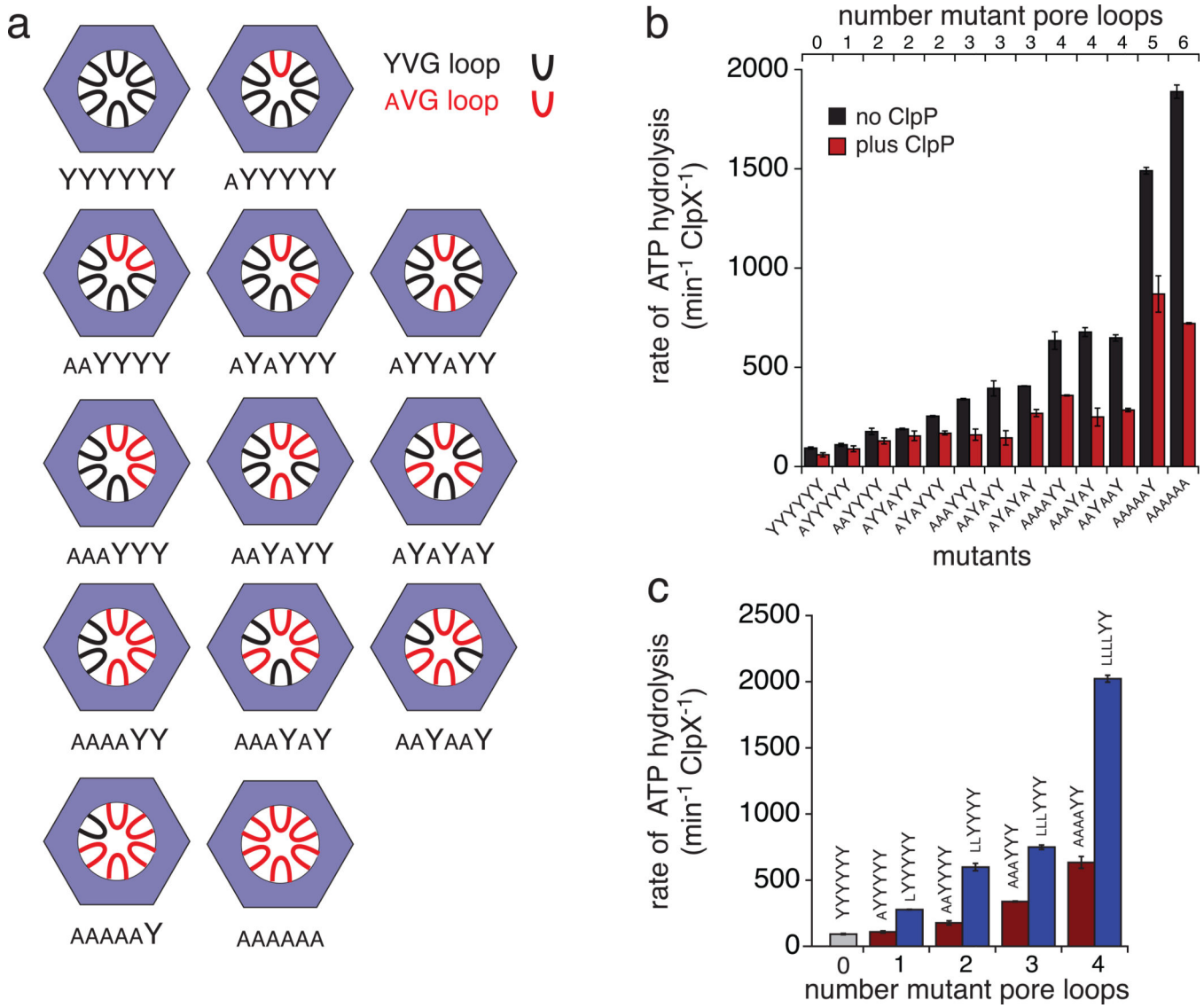

Figure 2.

Pore-loop mutants. (**a**) Arrangement of wild-type (YVG; black) and mutant (AVG; red) pore loops in the six subunits of covalently linked pseudo hexamers of ClpX. (**b**) Rates of ATP hydrolysis were measured for each pore-loop ClpX variant (100 nM) alone (dark blue) or in the presence of $ClpP_{14}$ (300 nM; light red). (**c**) Rates of ATP hydrolysis for ClpX variants (100 nM) with one to four adjacent Y153A (dark red) or Y153L (blue) pore-loop mutations in the absence of ClpP. Error bars in panels **b** and **c** are averages ($N \geq 3$) ± 1 standard deviation (SD).

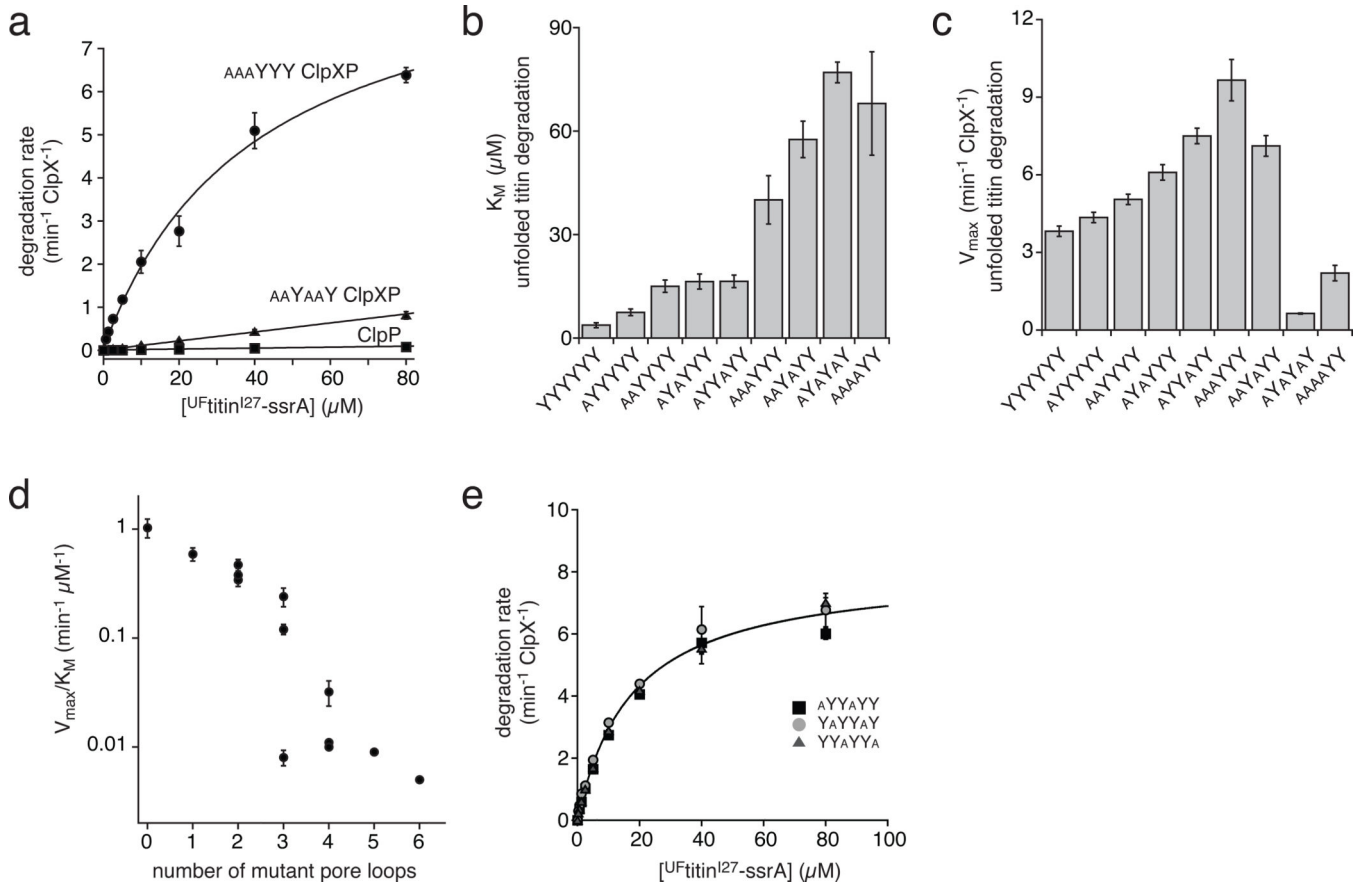

Figure 3.

Degradation of unfolded ^{UF}titin^{I27}-ssrA). (**a**) The substrate dependence of degradation rates by $_{AAA}$YYY ClpXP, $_{AA}$Y$_{AA}$Y ClpXP, and ClpP alone (200 nM ClpX variant; 300 nM ClpP) were fit to the Michaelis-Menten equation for $_{AAA}$YYY ClpXP and to a linear function for $_{AA}$Y$_{AA}$Y ClpXP and ClpP. Values are averages (N=3) ± 1 SD. (**b**) K_M values for degradation of ^{UF}titin^{I27}-ssrA were determined from the Michaelis-Menten plots in panel **a** and Supplementary Fig. 1. The error of non-linear least-squares fitting is shown. (**c**) V_{max} values and fitting errors for degradation of ^{UF}titin^{I27}-ssrA were determined from the Michaelis-Menten plots in panel **a** and Supplementary Fig. 1. (**d**) The second-order rate constant for ^{UF}titin^{I27}-ssrA ClpXP degradation (V_{max}/K_M) is plotted on a log scale as a function of the number of Y153A pore loop mutations in the ClpX hexamer. For variants with defined values of V_{max} and K_M, the error in V_{max}/K_M was propagated from the errors in individual parameters; for variants without defined values of V_{max} and K_M, the error is from linear fitting (Supplementary Fig. 1). (**e**) Degradation of ^{UF}titin^{I27}-ssrA by $_{A}$YY$_{A}$YY, Y$_{A}$YY$_{A}$Y, and YY$_{A}$YY$_{A}$ ClpXP (25 nM ClpX variant; 37.5 nM ClpP), which contain the same relative configuration of wild-type and mutant pore loops in different registers with respect to the N and C termini of the single-chain hexamer. Values are averages (N=3) ± 1 SD. The line is a fit of the combined data to the Michaelis-Menten equation (V_{max} = 8.1 ± 0.21 min^{-1} ClpX^{-1}; K_M = 17 ± 1.2 μM; R^2 = 0.99).

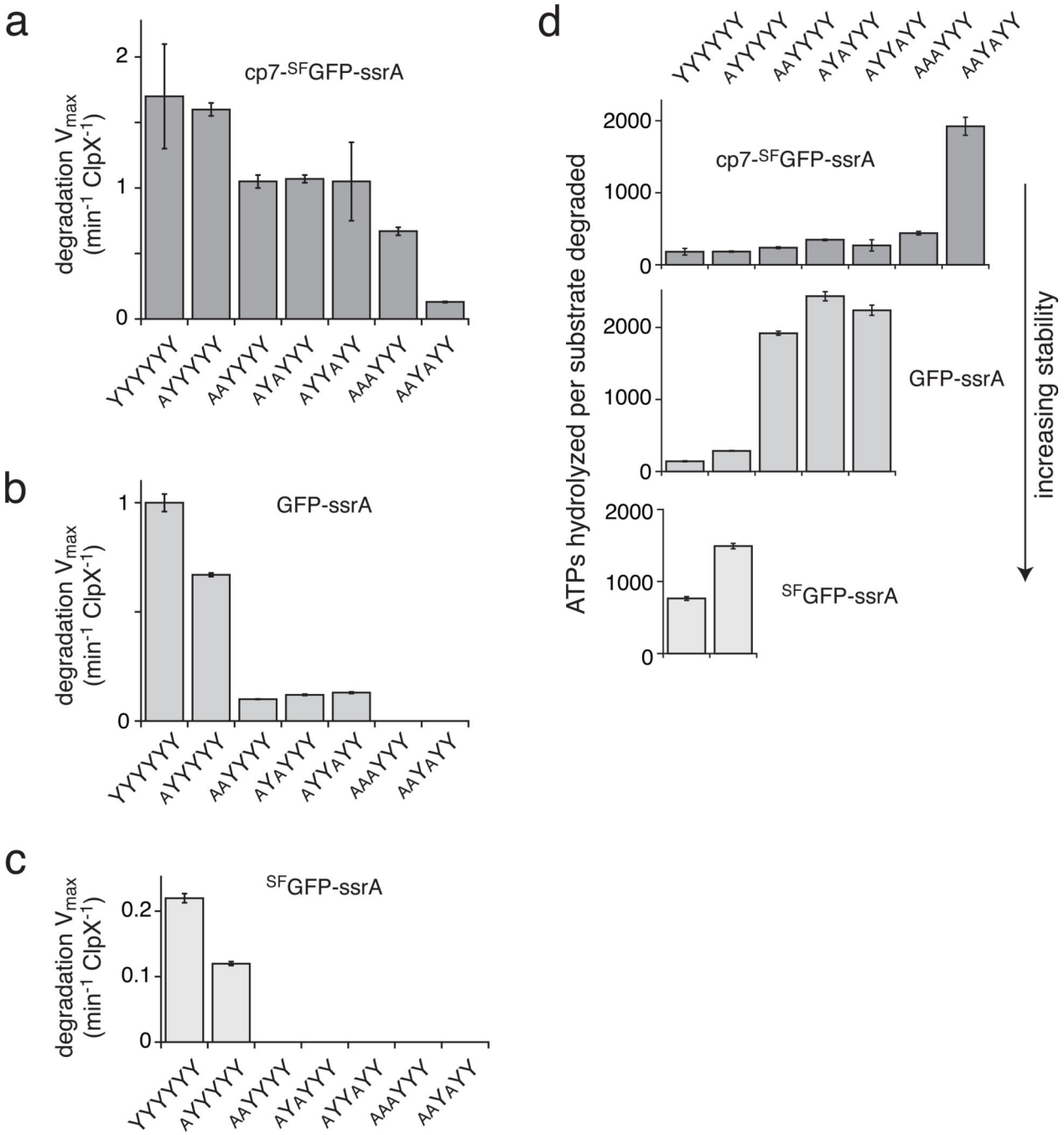

Figure 4.

Unfolding and degradation of native GFP substrates by pore-loop variants of ClpXP. (**a–c**) Maximal rates of degradation of cp7-^{SF}GFP-ssrA (**a**), GFP-ssrA (**b**), and ^{SF}GFP-ssrA (**c**) by the YYYYYY, $_{A}$YYYYY, $_{AA}$YYYY, $_{A}$YY$_{A}$YY, $_{A}$Y$_{A}$YYY, $_{AAA}$YYY, and $_{AA}$Y$_{A}$YY pore-loop ClpXP variants. For the enzymes that degraded these substrates, Michaelis-Menten plots are shown in Supplementary Fig. 4 and kinetic parameters are listed in Supplementary Table 2. (**d**) The ATP cost of degrading one molecule of native GFP substrates of increasing stability

increases as the number of wild-type pore loops decreases. In all panels, values are averages (N=3) ± 1 SD.

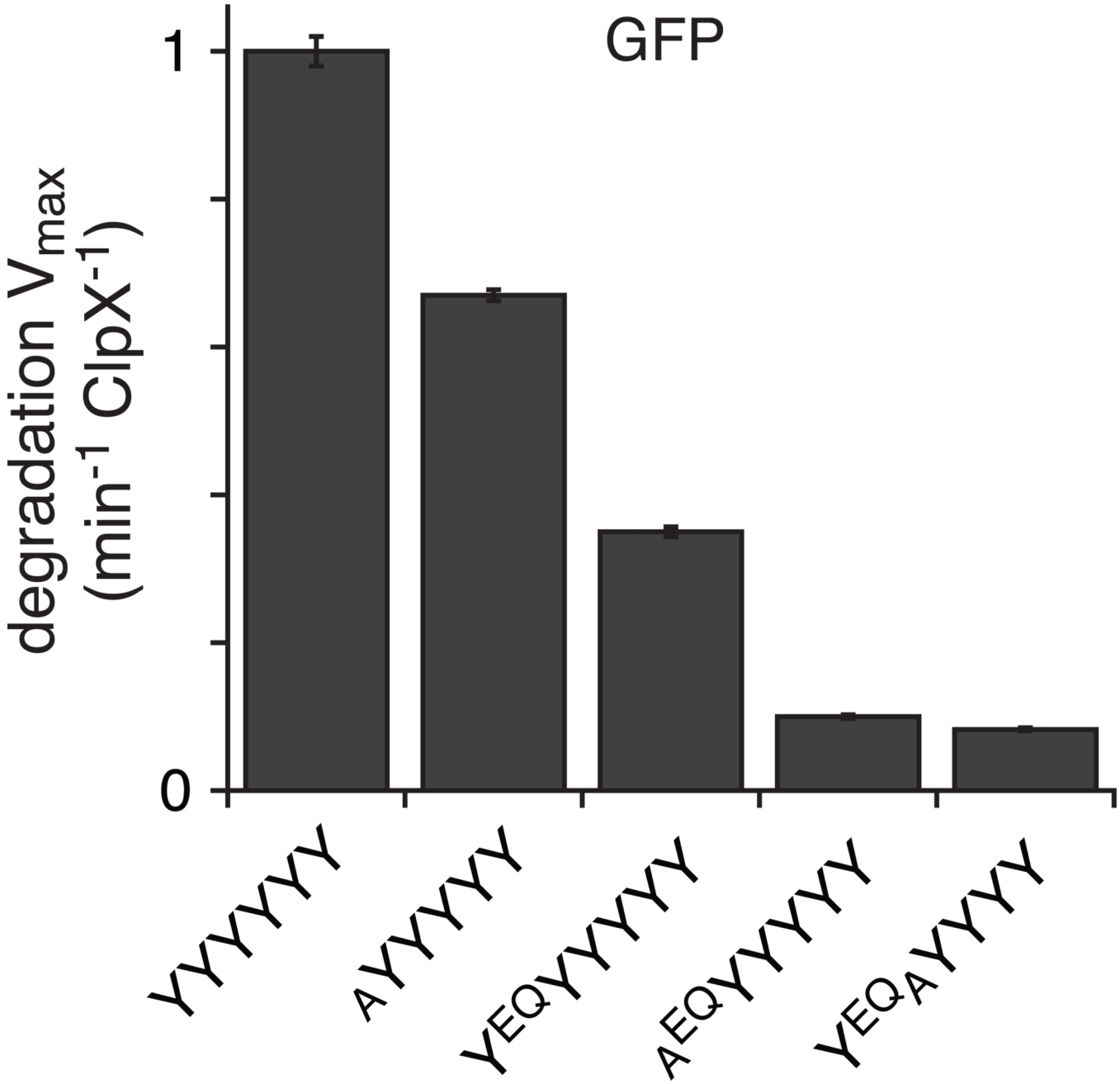

Figure 5.

Maximal rates of GFP-ssrA degradation by ClpXP variants containing one pore-loop mutation (A) and/or one ATP-hydrolysis mutation (EQ) in the same or different subunits supports a model in which the function of a pore-loop in one subunit is independent of ATP hydrolysis in the same subunit. Values are averages (N=3) ± 1 SD. Michaelis-Menten plots are shown in Supplementary Fig. 4.

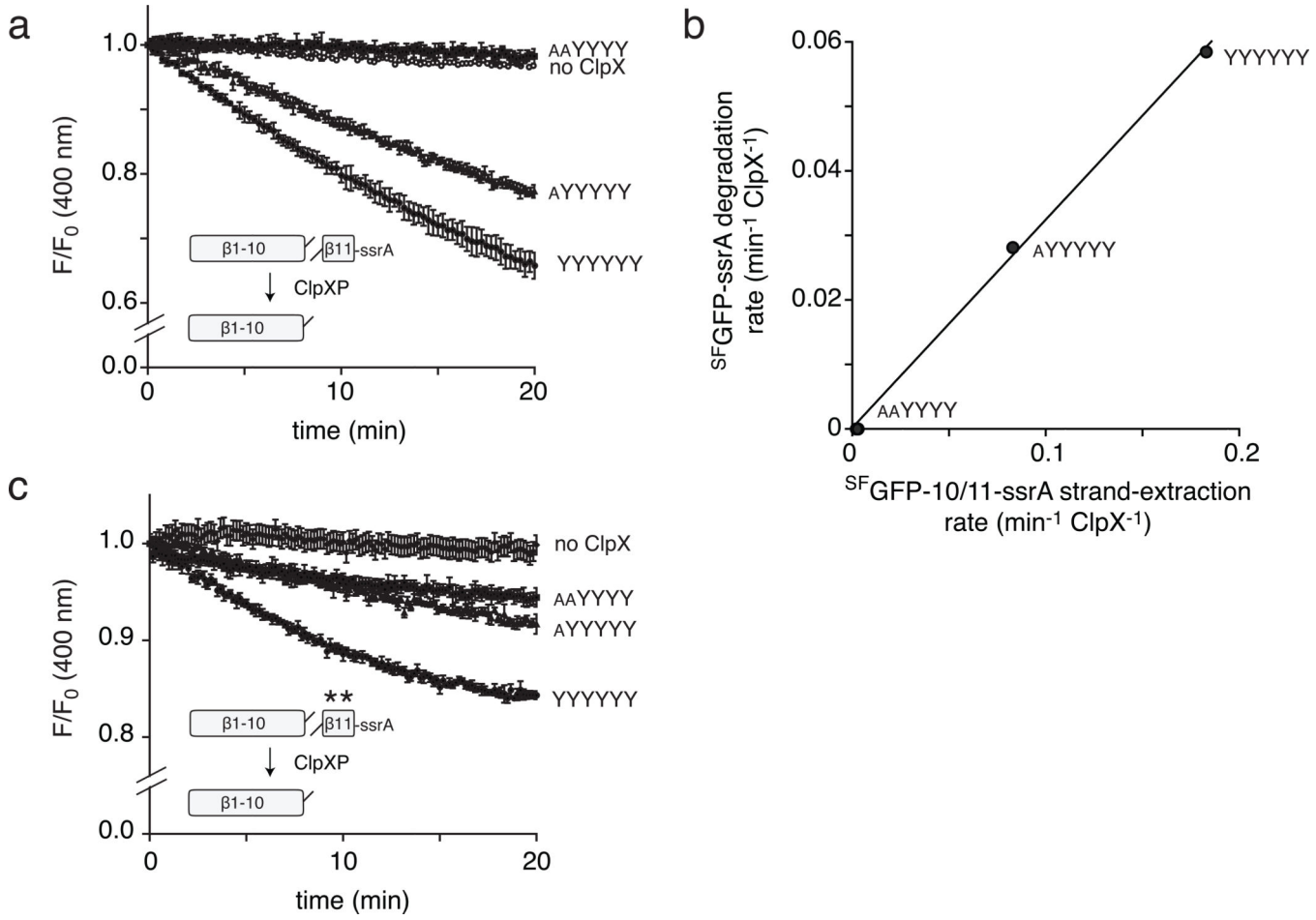

Figure 6.

Initiation of GFP-ssrA unfolding. (**a**) Extraction of the C-terminal β strand from thrombin-split ^{SF}GFP-10/11-ssrA (10 μM) by ClpX (0.3 μM) variants and ClpP (0.9 μM) was monitored by loss of fluorescence at 511 nm after excitation by 400-nm light[26]. Values are averages (N=4) ± 1 SD. (**b**) Correlation between the initial rate of strand extraction from thrombin-split ^{SF}GFP-10/11-ssrA (x-axis) and the rate of degradation of ^{SF}GFP-ssrA (y-axis). (**c**) Extraction of the C-terminal β strand from thrombin-split ^{SF}GFP-10/11-ssrA containing the F223A/A226G mutations in β11 (10 μM) by ClpX (0.3 μM) variants and ClpP (0.9 μM) was monitored as described in panel **a**. Values are averages (N=4) ± 1 SD. The final fluorescence in panels **a** and **c** is different and thus extraction rates cannot be directly compared.